FISEVIER

Contents lists available at ScienceDirect

Scripta Materialia

journal homepage: www.elsevier.com/locate/scriptamat



An alternative approach to predict Seebeck coefficients: Application to $La_{3-x}Te_4$



Yi Wang ^{a,*}, Xiaoyu Chong ^{a,*}, Yong-Jie Hu ^a, Shun-Li Shang ^a, Fivos R. Drymiotis ^b, Samad A. Firdosy ^b, Kurt E. Star ^b, Jean-Pierre Fleurial ^b, Vilupanur A. Ravi ^{b,c}, Long-Qing Chen ^a, Zi-Kui Liu ^a

- ^a Department of Materials Science and Engineering, The Pennsylvania State University, University Park, PA 16802, USA
- ^b Jet Propulsion Laboratory, California Institute of Technology, 4800 Oak Grove Drive, Pasadena, CA 91109, USA
- ^c Department of Chemical and Materials Engineering, California State Polytechnic University, Pomona, CA 91768, USA

ARTICLE INFO

Article history: Received 30 January 2019 Received in revised form 15 April 2019 Accepted 13 May 2019 Available online 24 May 2019

Keywords: Seebeck coefficient Electrochemical potential La3-xTe4 DFT Quasiharmonic

ABSTRACT

A thermodynamic understanding of Seebeck coefficient was demonstrated in terms of electrochemical potential. It divided the contributions to the Seebeck coefficient into two contributions: the effect of thermal electronic excitations due to Fermi distribution and the effect of charge carrier gradient due to thermal expansion. The procedure is illustrated within the rigid band approximation in terms of the electronic density-of-states and the quasiharmonic approximation in terms of the phonon density-of-states. Numerical results were given using the n-type high temperature thermoelectric material $\text{La}_{3-x}\text{Te}_4$ at x=0,0.25, and 0.33 as the prototype at a variety of carrier concentrations.

© 2019 Published by Elsevier Ltd on behalf of Acta Materialia Inc.

Thermoelectric materials [1–3] can be used to generate electricity, measure temperature or change the temperature of objects due to the reversible (see the review by Wood [4]) Seebeck effect, Peltier effect, or Thomson effect, each of which deals with the direct conversion of temperature differences at dissimilar metal junctions to electric voltage and vice versa [5–8]. A modern thermoelectric device is composed of ptype and *n*-type semi-conductors, which are coupled to the heat source through a hot shoe and the heat sink through the cold shoe. While the theory of the thermoelectric effect appears to be well established and widely applied in literature, the microscopic theory of thermoelectrics and the parameter-free calculation of thermoelectric properties remain challenging. This is particularly true for the calculation of the Seebeck coefficient. The Seebeck coefficient is also known as thermopower, thermoelectric power, or thermoelectric sensitivity and is defined as $S_a =$ $\Delta \phi / \Delta T$. It corresponds to the magnitude of an induced thermoelectric voltage, $\Delta \phi$, in response to a temperature difference, ΔT , across two points with different temperature within a material. Earlier theoretical descriptions of the Seebeck coefficient in terms of the differential electrical conductivity were given by Cutler and Mott [9], which were the foundation of later works [10–16] in terms of the transmission function [17–19] from the thermoelectric transport theory [20–22]. Recent studies [23-26] have noticed the possible relation between the Seebeck coefficient and system's chemical potential or the electrochemical

E-mail addresses: yuw3@psu.edu (Y. Wang), xuc83@psu.edu (X. Chong).

potential. Since the chemical potential and electrochemical potential are thermodynamic quantities, it makes it possible to calculate the Seebeck coefficient without using the concepts of relaxation time or mechanisms of electron and phonon scattering.

Let us start from the fundamental relation between the electrical current density ${\bf J}$ and the total potential (or total chemical potential), $\overline{\mu}$, seen by a charge carrier. Physically, $\overline{\mu}$ can be split into the internal chemical potential and the external chemical potential [27]. The external potential is the sum of the electric potential (voltage), gravitational potential (due to height, neglected in the present work), etc. The internal chemical potential includes everything else besides the external potentials, such as density, temperature, and enthalpy. According to classical mechanics, the net force felt by the charge carrier should equal to the negative gradient of the potential, i.e. $-\nabla \overline{\mu}$. This force can be rewritten as an effective electric field, $-\nabla \overline{\mu}/q$, where q represents the charge carried by the charge carrier. Hence, the electrical current can be written as:

$$\mathbf{J} = -\frac{1}{q} \mathbf{\sigma} \cdot \nabla \overline{\mu} \tag{1}$$

where σ is a tensor representing the electrical conductivity.

In generic terms, we can point out that $\overline{\mu}$ in Eq. (1) is exactly the electrochemical potential [28], per the definition that electrochemical potential is the mechanical work done in bringing 1 mol of charge carriers from a standard state to the considered system, according to International Union of Pure and Applied Chemistry [28]. For example,

Corresponding authors.

in the case of electrons as the charge carriers the electrochemical potential is the total potential, including both the internal chemical potential and the electric potential, and it is by definition constant across a device in equilibrium. Whereas, the chemical potential of electrons is equal to the electrochemical potential minus the local electric potential energy per electron. As a result $\overline{\mu}$ is the partial molar Gibbs energy of the charge carriers and can be expressed as

$$\overline{\boldsymbol{\mu}} = \boldsymbol{\mu} + \boldsymbol{q} \, \boldsymbol{\varphi}' \tag{2}$$

where μ represents the internal chemical potential of the considered charge carrier under zero external electric field and φ' represents local electrical potential due to an external field.

In the case of a thermoelectric device, since there are no any moving parts, except the moving charge carriers, the change in μ due to a temperature difference must be the only reason behind the thermoelectric electromotive force. Therefore, one ought to separate μ into the combinations of temperature (T) dependent part, $\zeta = \mu - \varepsilon_F(V)$ (following the notation given by Sommerfeld [29]) which equals to zero at T=0, and the volume (V) dependent only part, $\varepsilon_F(V)$ which is the Fermi energy (i.e., the value of μ at 0 K) at the same volume. Accordingly, we can rewrite Eq. (2) as

$$\overline{\mu} = \zeta + q \, \phi \tag{3}$$

where $\phi = \phi' + \varepsilon_F/q$ implying the 0 K contribution has been merged with ϕ' . Inspired by the concept of absolute thermal electric force defined by Ziman [30], correspondingly, we may call ϕ as the absolute voltage.

In the meantime, for formulating thermoelectric effects, ${\bf J}$ is usually expressed as.

$$\mathbf{J} = -\frac{1}{q} \sigma \cdot \left(-\nabla \varphi + \mathbf{S}_q \cdot \nabla T \right) \tag{4}$$

where $\nabla \varphi$ represents the local electric field purely due to the electric/electrostatic potential φ and \mathbf{S}_a is Seebeck coefficient.

We can point out that φ in Eq. (4) and ϕ in Eq. (3) are the same quantity since they are due to the presence of an external field. Consequently, combining Eq. (3) with Eq. (1) and comparing with Eq. (4), returns:

$$\mathbf{S}_q = -\frac{1}{q} \frac{\nabla \zeta}{\nabla T}.\tag{5}$$

In general, S_q defined from Eq. (5) is a tensor.

Next, we treat the dependence of ζ on the gradients of both electrical charge carrier density (n) and temperature by writing

$$\nabla \zeta = \left(\frac{\partial \zeta}{\partial n}\right)_T \nabla n + \left(\frac{\partial \zeta}{\partial T}\right)_V \nabla T. \tag{6}$$

We note that the electric field inside a conductor is zero by Gauss's law [31]. This is true under the open circuit condition under which the Seebeck coefficient is measured [32,33]. i.e., there is no net charge inside a conductor and this is true in the case of uniform electric field. Therefore, the change in n is solely due to the change in volume through

$$n = \frac{N}{V} \tag{7}$$

where N is the number of electrons in the considered system, knowing the fact that the charges of the electrons are always balanced by the nuclear charges under the conditions of zero net charge. Inserting Eq. (7) into Eq. (6) returns:

$$\nabla \zeta = \left(\frac{\partial \zeta}{\partial V}\right)_T \nabla V + \left(\frac{\partial \zeta}{\partial T}\right)_V \nabla T. \tag{8}$$

As a result, when the electrons are explicitly treated as the charge carriers (q = -e where e is the elementary charge), combining Eqs. (5) and (8) gives:

$$\mathbf{S}_{e} = \frac{1}{e} \left[\left(\frac{\partial \zeta}{\partial V} \right)_{T} \frac{\nabla V}{\nabla T} + \left(\frac{\partial \zeta}{\partial T} \right)_{V} \right]. \tag{9}$$

Finally, in the case of an isotropic system $\frac{\nabla V}{\nabla T}$ can be replaced by the volume thermal expansion at constant pressure (*P*). Hence Eq. (9) becomes:

$$S_{e} = \frac{1}{e} \left[\left(\frac{\partial \zeta}{\partial V} \right)_{T} \left(\frac{\partial V}{\partial T} \right)_{P} + \left(\frac{\partial \zeta}{\partial T} \right)_{V} \right]$$
 (10)

From Eq. (10), it can be seen that the constant pressure Seebeck coefficient contains two terms: The first term $\left(\frac{\partial \zeta}{\partial V}\right)_T$, $\left(\frac{\partial V}{\partial T}\right)_P$ is due to

the thermal expansion, whereas the second term $\left(\left(\frac{\partial \zeta}{\partial T}\right)_V\right)$ accounts

for the constant volume contribution. Once the electronic density of states (e-DOS) has been calculated from first-principles [34–36], the calculation of ζ is straightforward. The calculation can be performed based on Mermin's finite temperature density functional theory [37,38] and it has been demonstrated in previous work [26]. Considering the fact that the electrons are explicitly treated in the current implementation [39,40] of first-principles calculations, i.e. $q=-e, \zeta$ in Eq. (3) should obey the Fermi-Dirac distribution

$$f = \frac{1}{\exp\left[\frac{\varepsilon - \zeta}{k_B T}\right] + 1} \tag{11}$$

where the Fermi energy has been taken as the reference for the band energy ε . In such a way, ζ is determined by the conservation equation

$$\int n(\varepsilon, V) f d\varepsilon = N \tag{12}$$

where $n(\varepsilon,V)$ is the electronic density of states (e-DOS), N is the total number of electrons in the system.

The demonstration of the theory is given below using the n-type thermoelectric material La_{3-x}T₄, whose thermodynamic properties have been calculated in our recent publication [41] using the quasiharmonic phonon approach [42,43]. In particular, we have utilized the calculated e-DOS and thermal expansion using the Perdew-Burke-Ernzerhof revised for solids (PBEsol) [44] exchange-correlational functional, obtained from the projector-augmented wave (PAW) method [39,40] as implemented in the Vienna ab initio simulation package (VASP, version 5.3). Spin-orbit interactions are not considered.

The temperature dependence of ζ is solely dictated by the behavior of the e-DOS by the present formalism, and so is the Seebeck coefficient. The faster the change of the e-DOS in the vicinity of the Fermi energy with respect to the band energy, the faster of the change of ζ with respect to temperature, and the larger the Seebeck coefficient. This is in agreement with [45], but not limited to, the concept of convergence band [2,46]. Numerically, the rapid increase of the e-DOS with increasing band energy is the reason ζ decreases with increasing temperature, resulting in a negative Seebeck coefficient for La_{3-x}Te₄.

Typically for a n-type semiconductor, the chemical potential of electrons at 0 K (Fermi energy) is located slightly above the bottom of the conduction band, as shown in Fig. 1 (in the case of La_3Te_4 and $La_{2.75}Te_4$). For an insulator, the Fermi energy is located at the top of

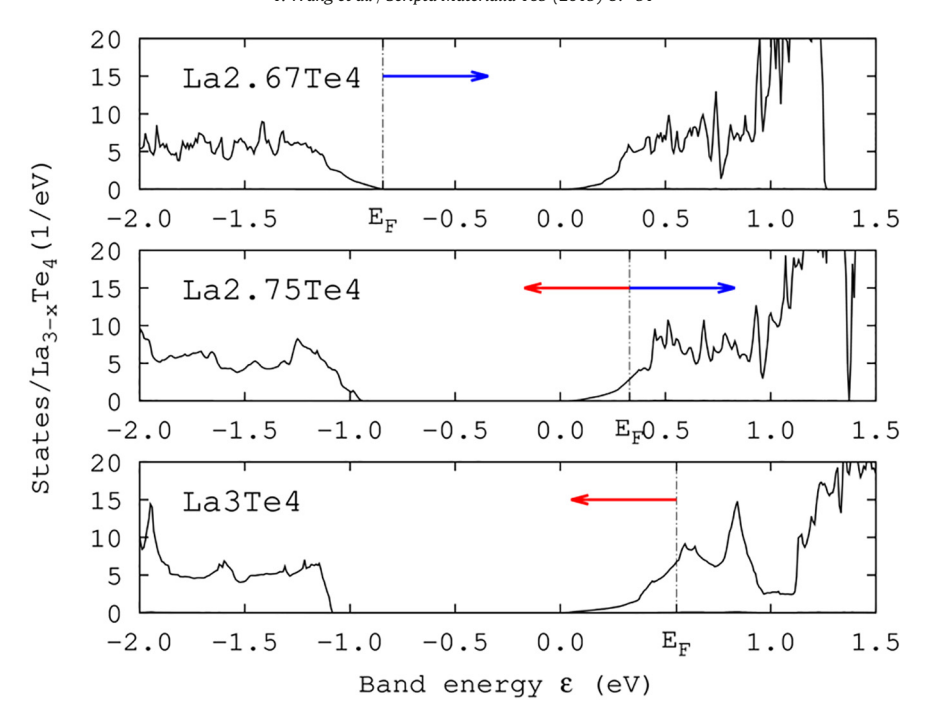


Fig. 1. Calculated electronic density-of-states for La_3Te_4 , $La_{2.75}Te_4$, and $La_{2.67}Te_4$. The vertical dot-dashed lines with label " E_F " indicate the Fermi energies (ε_F as defined by the explanation of Eq. (3)) without doping. The arrows label the possible types of doping for the three referenced compositions.

the valence band, as shown in Fig. 1 for $La_{2.67}$ Te₄. The criteria for a good n-type semiconductor can be described as follows:

- i) at 0 K, relatively low values of e-DOS at the Fermi energy which in turn is located at slightly above the bottom of the conduction band, as shown in the plot of the e-DOS for $La_{2.75}Te_4$ in Fig. 1; and
- ii) the e-DOS increases rapidly with the increasing values for the electron band energy.

Consequently, the Seebeck coefficient can be calculated directly with one-dimensional numerical integration. Since the e-DOS is a basic output of most modern first-principles codes, the present formulation makes it a lot easier to search for superior thermoelectric materials by means of high-throughput first-principles calculations [35,36].

Next, we will discuss in detail the first-principles calculations of the temperature dependence of the Seebeck coefficients for Lanthanum

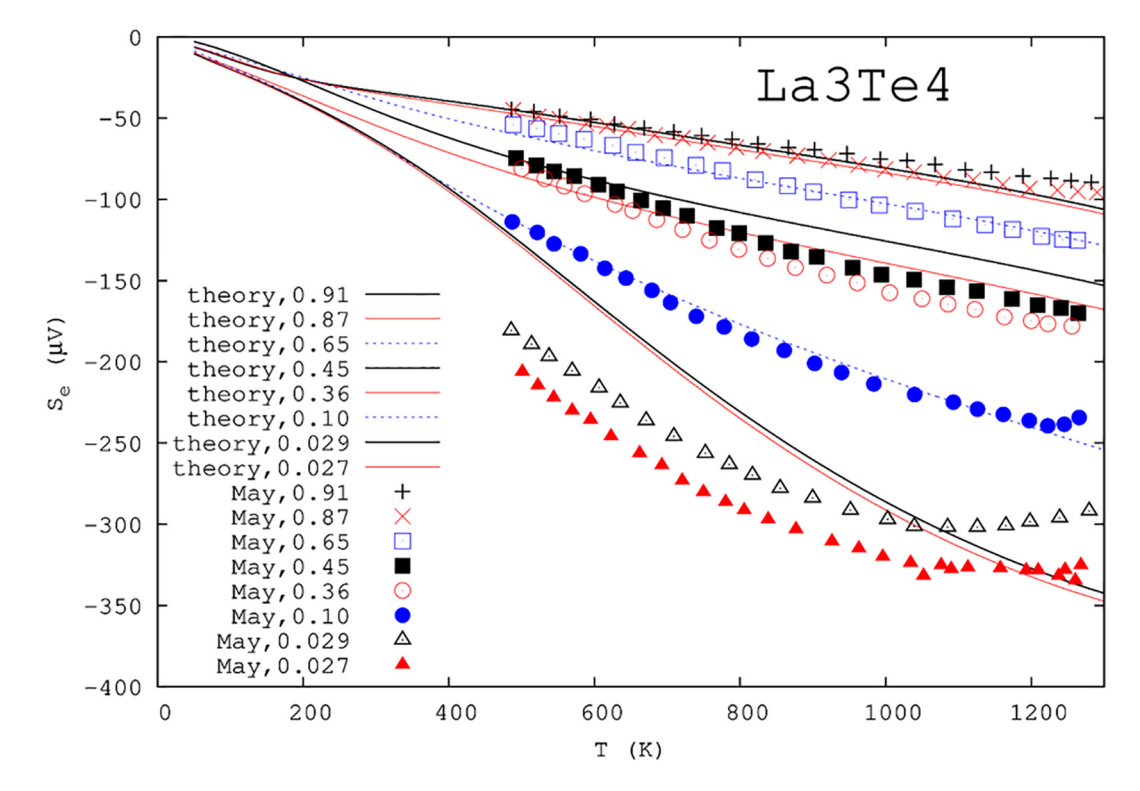


Fig. 2. Calculated Seebeck coefficients for La_{3-x}Te₄ based on the electronic density-of-states of La₃Te₄. The carrier concentrations of 4.0×10^{21} , 3.8×10^{21} , 2.9×10^{21} , 2.0×10^{21} , 1.6×10^{21} , 4.6×10^{21} , 4.4×10^{20} , and 4.2×10^{20} , and 4.2×10^{20} e/cm³ correspond to the reduced Hall carrier concentrations of 0.91, 0.87, 0.65, 0.45, 0.36, 0.10, 0.029, and 0.027, respectively, from the experiments by May et al. [47].

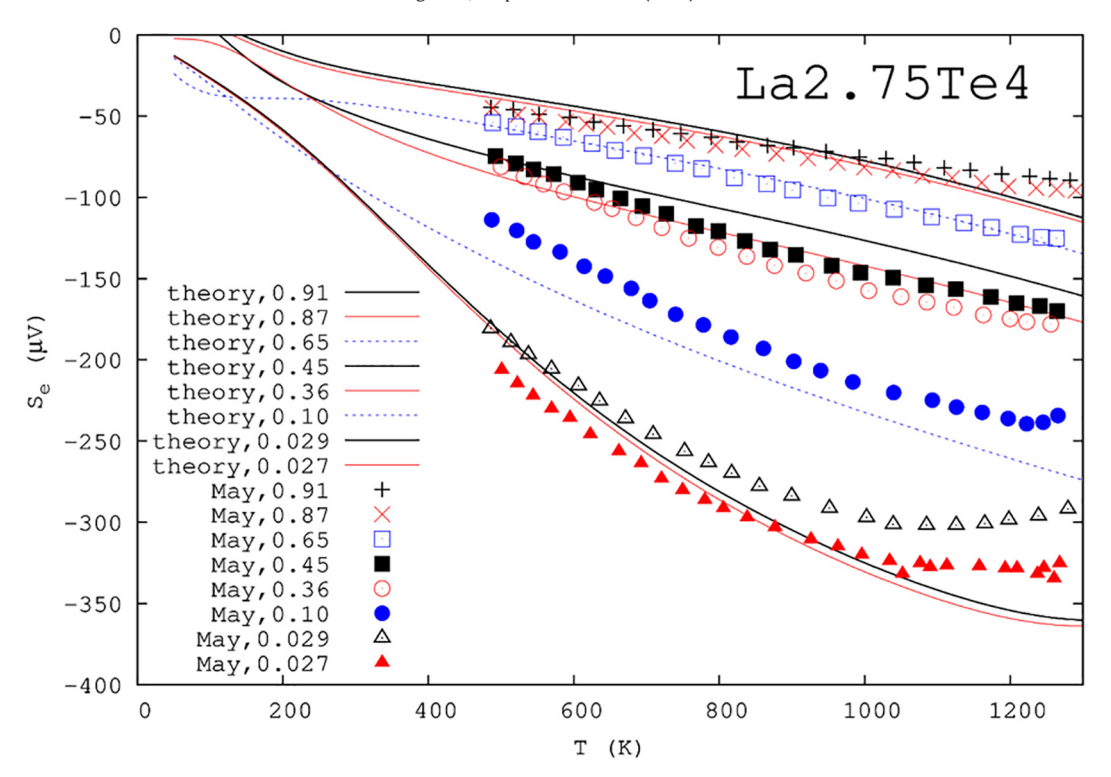


Fig. 3. Calculated Seebeck coefficients for $L_{3...}$ Te₄ based on the electronic density-of-states of $L_{2.75}$ Te₄. The carrier concentration of 4.0×10^{21} , 3.8×10^{21} , $2.9 \times$

telluride ($La_{3-x}Te_4$) in order to demonstrate the proposed formalism. $La_{3-x}Te_4$ is used for thermoelectric power generation under the high temperature environment. A thermoelectric material is often characterized by the carrier concentration, i.e., the number of electrons in the

conduction band (or the number of holes in the valence band) which are mostly implemented by doping the perfect crystal. In principle, a precise first-principles calculation should be performed using the doped structure. However, doing so is often very time consuming. An

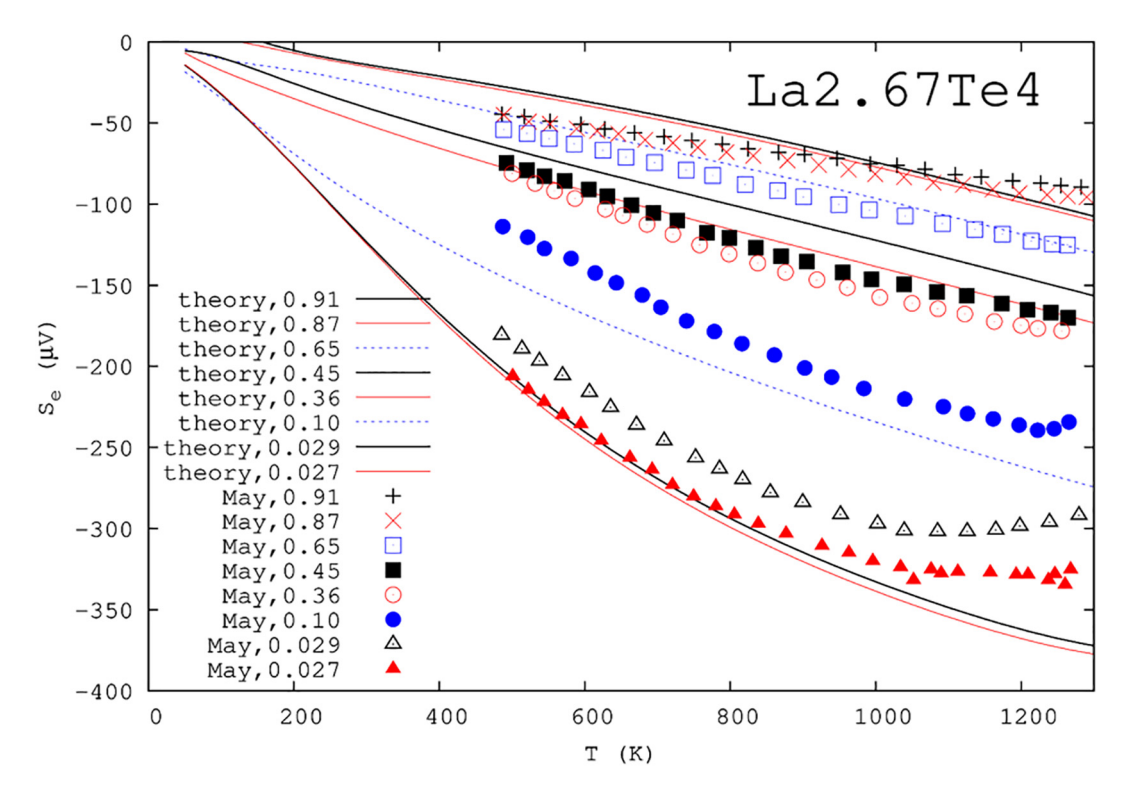


Fig. 4. Calculated Seebeck coefficients for La_{3-x}Te₄ based on the electronic density-of-states of La_{2.67}Te₄. The carrier concentration of 4.0×10^{21} , 3.8×10^{21} , 2.9×10^{21} , 2.0×10^{21} , 1.6×10^{21} , 1.6×10^{21} , 1.6×10^{21} , 1.3×10^{20} , and 1.2×10^{20} e/cm³ correspond to the reduced Hall carrier concentrations of 0.91, 0.87, 0.65, 0.45, 0.36, 0.10, 0.029, and 0.027, respectively, from the experiments by May et al. [47].

alternative solution is to adopt the rigid band approximation [22]. In this approximation, the electronic band structure is first calculated for a reference crystal structure. The electronic band structure is subsequently assumed to remain unchanged, but the Fermi energy is adjusted to fit the desired carrier concentrations. In order to study the effects of different reference crystal structures on the calculated Seebeck coefficients, we have considered the following three cases: La₃Te₄, La_{2.75}Te₄, and La_{2.67}Te₄.

From the viewpoint of chemical valence, the cation La has a valence +2, and anion Te has a valence of -3. It can therefore be anticipated that a vacancy at the La site can transform the material from a metal at x = 0 to an insulator at x = 1/3, knowing the fact that La₃Te₄ has one electron located at the conduction band, and La_{2.67}Te₄ has no electron located at the conduction band. We consider a variety of carrier concentrations of 4.0×10^{21} , 3.8×10^{21} , 2.9×10^{21} , 2.0×10^{21} , 1.6×10^{21} , 4.4×10^{20} , 1.3×10^{20} , and 1.2 \times 10²⁰ e/cm³. These carrier concentrations correspond to the reduced Hall carrier concentrations of $\eta_H = 0.91, 0.87, 0.65, 0.45,$ 0.36, 0.10, 0.029, and 0.027, respectively, given in the measurements made by May et al. [47]. Effectively, La₃Te₄ corresponds to $\eta_H = 1$ and La_{2.67}Te₄ corresponds to $\eta_H = 0$.

Based on the calculated e-DOS as shown in Fig. 1, the different carrier concentrations can be implemented by removing electrons from or adding electrons into the reference structures, i.e., changing the value of N in the right hand side of Eq. (12). The particular procedure corresponds to removing electrons from La₃Te₄, adding electrons to La_{2.67}Te₄, adding electrons to La_{2.75}Te₄ for high carrier concentrations $(\eta_H = 0.91, 0.87, 0.65, 0.45, \text{ and } 0.36)$, and removing electrons from $La_{2.75}Te_4$ for low carrier concentrations $\eta_H = 0.10$, 0.029, and 0.027. Consequently, the change in carrier concentration will result in new Fermi energy (ε_F) as defined in Eq. (3). The Seebeck coefficients are subsequently calculated using Eq. (10), depending on the referenced structure (La₃Te₄, La_{2.75}Te₄, and La_{2.67}Te₄).

The three sets of Seebeck coefficients calculated based on three referenced crystal structures of La₃Te₄, La_{2.75}Te₄, and La_{2.67}Te₄, are compared with the experimental data for La_{3-x}Te₄ by May et al. [47] superimposed in Figs. 2, 3, and 4, respectively. Good agreement with experiment using La₃Te₄ as the referenced structure for high carrier concentration (knowing La₃Te₄ is almost a good conductor as seen from Fig. 1). Good agreement with experiment using La_{2.67}Te₄ as the referenced structure for low carrier concentration (knowing La_{2.67}Te₄ is insulator as seen from Fig. 1). The modest deviations between the calculations and experiments for lower carrier concentrations at $\eta_H =$ 0.10, 0.029, and 0.027 can be in part attributed to the experimental difficulties, due to reasons such as sample inhomogeneity and oxidation [47]. This is particularly true as it is seen that the calculated difference at $\eta_H = 0.029$ and 0.027 is one magnitude smaller than the measured one by May et al. The difference between the Seebeck coefficients at $\eta_H = 0.029$ and 0.027 should not have been as large as that reported from the overall good agreements between the calculations and experiments in the whole carrier concentration range between 0.91 and 0.027. As discussed by May et al., when approaching to the insulating limit of the stoichiometric La_{2.67}Te₄, the uncertainty associated with electrical resistivity and Seebeck coefficient is considerably large. It was seen that the measured Hall carrier concentrations showed ~10% uncertainties against the nominal vacancy concentration (i.e. the value of x in La_{3-x}Te₄) and the Hall carrier concentrations were slightly underestimated for larger x (i.e. small η_H).

Acknowledgements

The research was carried out at the Jet Propulsion Laboratory, California Institute of Technology and The Pennsylvania State University, under a contract with the National Aeronautics and Space Administration. This work was also supported by National Science Foundation (NSF) through Grant No. CMMI-1825538 (Wang, Shang, and Liu) and

by NSF through Grant No. DMR-1744213 (Wang and Chen). This research received funding from the Pennsylvania State University's Institute for CyberScience through the ICS Seed Grant Program (Wang, Liu, and Chen). First-principles calculations were carried out partially on the LION clusters at the Pennsylvania State University supported by the Materials Simulation Center and the Research Computing and Cyberinfrastructure unit at the Pennsylvania State University, partially on the resources of NERSC supported by the Office of Science of the US Department of Energy under contract No. DE-AC02-05CH11231, and partially on the resources of Extreme Science and Engineering Discovery Environment (XSEDE) supported by NSF with Grant No. ACI-1548562.

References

- [1] K. Biswas, J. He, I.D. Blum, C.-I. Wu, T.P. Hogan, D.N. Seidman, V.P. Dravid, M.G. Kanatzidis, Nature 489 (2012) 414-418.
- Y. Pei, X. Shi, A. LaLonde, H. Wang, L. Chen, G.J. Snyder, Nature 473 (2011) 66-69.
- J. Yang, L. Xi, W. Qiu, L. Wu, X. Shi, L. Chen, Npj Comput. Mater. 2 (2016), 15015.
- C. Wood, Rep. Prog. Phys. 51 (1988) 459.
- C. Goupil, W. Seifert, K. Zabrocki, E. Müller, G.J. Snyder, Entropy 13 (2011) 1481-1517
- G.I. Snyder, E.S. Toberer, Nat. Mater, 7 (2008) 105-114.
- I. Vaskivskyi, J. Gospodaric, S. Brazovskii, D. Svetin, P. Sutar, E. Goreshnik, I.A. Mihailovic, T. Mertelj, D. Mihailovic, Sci. Adv. 1 (2015), e1500168.
- W.G. Zeier, J. Schmitt, G. Hautier, U. Aydemir, Z.M. Gibbs, C. Felser, G.J. Snyder, Nat. Rev. Mater. 1 (2016), 16032.
- M. Cutler, N.F. Mott, Phys. Rev. 181 (1969) 1336.
- J.E. Parrott, IEEE Trans. Electron Devices 43 (1996) 809-826
- G.K.H. Madsen, D.J. Singh, Comput. Phys. Commun. 175 (2006) 67-71.
- U. Sivan, Y. Imry, Phys. Rev. B 33 (1986) 551.
- P. Reddy, S.-Y. Jang, R.A. Segalman, A. Majumdar, Science (80-.) 315 (2007)
- L. Gravier, S. Serrano-Guisan, F. Reuse, J.-P. Ansermet, Phys. Rev. B 73 (2006), 24419.
 - M. Jonson, G.D. Mahan, Phys. Rev. B 21 (1980) 4223.
- M. Jonson, G.D. Mahan, Phys. Rev. B 42 (1990) 9350.
- C.R. Proetto, Phys. Rev. B 44 (1991) 9096.
- X. Zheng, W. Zheng, Y. Wei, Z. Zeng, J. Wang, J. Chem. Phys. 121 (2004) 8537–8541.
- Y.-S. Liu, Y.-C. Chen, Phys. Rev. B 79 (2009), 193101.
- [20] J.-C. Zheng, Front. Phys. China 3 (2008) 269-279.
- L.D. Hicks, M.S. Dresselhaus, Phys. Rev. B 47 (1993) 12727.
- T.J. Scheidemantel, C. Ambrosch-Draxl, T. Thonhauser, J.V. Badding, J.O. Sofo, Phys. Rev. B 68 (2003), 125210.
- Y. Apertet, H. Ouerdane, C. Goupil, P. Lecoeur, Eur. Phys. J. Plus 131 (2016) 1-8.
- S. Datta, Quantum Transport: Atom to Transistor, Cambridge University Press, 2005.
- M.R. Peterson, B.S. Shastry, Phys. Rev. B 82 (2010), 195105.
- Y. Wang, Y.-J. Hu, B. Bocklund, S.-L. Shang, B.-C. Zhou, Z.-K. Liu, L.-Q. Chen, Phys. Rev. B 98 (2018) 224101.
- C. Kittel, H. Kroemer, Thermal Physics, W.H. Freeman, 1980.
- A.D. McNaught, A. Wilkinson, International Union of Pure and Applied Chemistry, Compendium of Chemical Terminology: IUPAC Recommendations, Blackwell Sci-
- A. Sommerfeld, Thermodynamics and Statistical Mechanics, Academic Press, 1964. J.M. Ziman, Electrons and Phonons: The Theory of Transport Phenomena in Solids, Clarendon Press, 1960.
- E.M. Purcell, Electricity and Magnetism, Third edition Cambridge University Press, Cambridge; New York, 2013.
- [32] L. Adnane, N. Williams, H. Silva, A. Gokirmak, Rev. Sci. Instrum. 86 (2015), 105119.
- J. Martin, T. Tritt, C. Uher, J. Appl. Phys. 108 (2010) 121101.
- A. Jain, S.P. Ong, G. Hautier, W. Chen, W.D. Richards, S. Dacek, S. Cholia, D. Gunter, D. Skinner, G. Ceder, K.A. Persson, APL Mater. 1 (2013), 11002.
- S.P. Ong, W.D. Richards, A. Jain, G. Hautier, M. Kocher, S. Cholia, D. Gunter, V.L. Chevrier, K.A. Persson, G. Ceder, Comput. Mater. Sci. 68 (2013) 314-319.
- S. Bhattacharya, G.K.H. Madsen, Phys. Rev. B 92 (2015), 85205.
- A.K. McMahan, M. Ross, Phys. Rev. B 15 (1977) 718.
- N.D. Mermin, Phys. Rev. 137 (1965) A1441.
- G. Kresse, J. Furthmüller, Comput. Mater. Sci. 6 (1996) 15-50.
- [40] G. Kresse, D. Joubert, Phys. Rev. B 59 (1999) 1758-1775.
- Y. Wang, Y.-J. Hu, X. Chong, J.P.S. Palma, S.A. Firdosy, K.E. Star, J.-P. Fleurial, V.A. Ravi, S.-L. Shang, L.-Q. Chen, Z.-K. Liu, Comput. Mater. Sci. 142 (2018) 417-426.
- Y. Wang, J.J. Wang, W.Y. Wang, Z.G. Mei, S.L. Shang, L.Q. Chen, Z.K. Liu, J. Physics-Condensed Matter 22 (2010) 202201.
- [43] Y. Wang, S.-L. Shang, H. Fang, Z.-K. Liu, L.-Q. Chen, Npj Comput. Mater. 2 (2016), 16006.
- [44] J.P. Perdew, A. Ruzsinszky, G.I. Csonka, O.A. Vydrov, G.E. Scuseria, L.A. Constantin, X. Zhou, K. Burke, Phys. Rev. Lett. 100 (2008), 136406.
- [45] A.F. May, D.J. Singh, G.J. Snyder, Phys. Rev. B 79 (2009), 153101.
- [46] G.D. Mahan, J.O. Sofo, Proc. Natl. Acad. Sci. 93 (1996) 7436–7439.
- [47] A.F. May, J.-P. Fleurial, G.J. Snyder, Phys. Rev. B 78 (2008), 125205.